Biaxially Textured Al Film Growth on CaF_2 Nanostructures toward a Method of Preparing Single-Crystalline Si Film on Glass Substrates

Huafang Li,* Patrick Snow, Ming He, Pei-I Wang,* Gwo-Ching Wang, and Toh-Ming Lu

Department of Physics, Applied Physics and Astronomy, and Center for Integrated Electronics, Rensselaer Polytechnic Institute, 110 Eighth Street, Troy, New York 12180-3590

ABSTRACT We report the room temperature growth of biaxially textured Al films and further demonstrate the use of these Al films in preparing single-crystalline Si layers on glass substrates. The formation of the biaxial texture in Al film relies on the existence of the CaF_2 buffer layer prepared using oblique angle physical vapor deposition, which consists of single-crystalline nanorods with caps that are in the form of inverted nanopyramids. The single-crystalline Si film was obtained upon crystallization of the amorphous Si film deposited through physical evaporation on the biaxially textured Al film. This method of preparing single-crystalline Si film on glass substrate is potentially attractive for being employed in silicon technology and in fabrication of low-cost electronic devices.

KEYWORDS: nanoepitaxy · silicon technology · oblique angle deposition · solid phase transformation · physical vapor deposition · transmission electron microscopy

Recently, there has been considerable interest in the growth of biaxially crystallographic textured films on glass and flexible substrates because these films can serve further as substrates to grow biaxially textured superconductor films as well as to grow biaxial semiconductor films, such as Si, CdTe, and Ge, for potential low-cost solar cell applications.[1−13] The idea was based on the facts that (a) the biaxially crystallographic textured films can have comparable properties to their single-crystalline counterparts, and (b) the glass or flexible substrates, such as metal tapes and polymer sheets, can be less costly than single-crystalline wafers. To date, the biaxial films grown directly on the substrates without preferred orientation can be obtained by inclined substrate deposition (also known as oblique angle deposition, OAD) and ion bombardment deposition.[1−5,8,10,14−16] Using these techniques, the films of a few materials, including MgO,[1−6] CaF_2,[17] and β-W,[18] have so far been prepared and reported to exhibit good biaxial texture. However, films of other materials prepared using the same techniques have shown either no obvious biaxial texture or a texture with large angular spread. Heteroepitaxy is an alternative strategy to produce textured films that target specific applications. This approach has been utilized to prepare textured $YBa_2Cu_3O_x$ films on MgO through multiple buffer layers,[1−6] Si on MgO with γ-Al_2O_3 template layer,[10] CdTe on CaF_2,[11,12] and Ge on CaF_2.[13] There has been great interest in growing Si, the major material in the semiconductor industry, as a textured film. It is also preferable that the processing condition can be low temperature and low cost. Although Si has small lattice mismatch (~1%) with CaF_2, the growth through physical vapor deposition methods requires substrate temperature (>600 °C) higher than that which glass substrates and CaF_2 nanostructures can withstand, in order to get good quality crystalline films. Aluminum-induced crystallization has been found to reduce the processing temperature substantially so that crystalline Si film can be obtained at a temperature below 600 °C.[19−22] Meanwhile, Al has been known for decades to grow epitaxially on single-crystalline Si and CaF_2 substrates in high quality despite their large lattice mismatch (~25%).[23−25] Therefore, by the heteroepitaxy of the Al intermediate (or catalyst) layer on the biaxially textured CaF_2 nanostructures deposited on glass or flexible substrates, one can potentially increase the varieties of the materials to grow into biaxially textured films from these non-single-crystalline substrates. In this work, we report the biaxially textured Al film grown at room temperature on glass substrate using CaF_2 nanostructures as the buffer layer and the application of this

*Address correspondence to lih3@rpi.edu, wangp3@rpi.edu.

Received for review May 28, 2010 and accepted September 07, 2010.

Published online September 14, 2010.
10.1021/nn1011978

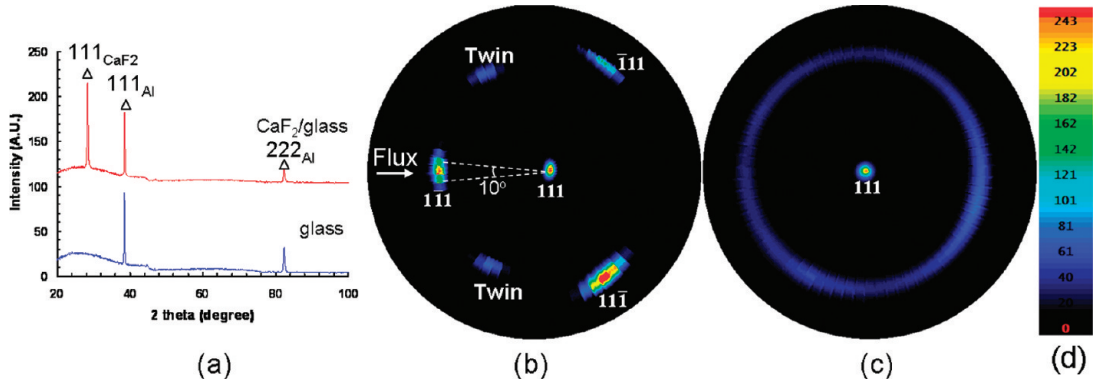

Figure 1. X-ray diffraction analyses of Al films grown on glass substrates with and without a biaxially textured CaF_2 buffer layer: (a) 2θ scan; (b) Al (111) pole figure of the film grown with a biaxially textured CaF_2 buffer layer; (c) Al (111) pole figure of the film grown directly on glass. (d) Color bar indicating the pole concentration in (b) and (c).

Al film to prepare a near single-crystalline Si film through crystallization at a temperature below 600 °C.

RESULTS AND DISCUSSION

Corning 2947 microscopy slides were used as substrates in this study. The CaF_2 buffer layer was thermally evaporated onto the glass slides.[17] It consists of a nanorod array with a homoepitaxially grown capping layer. The nanorod array is to ensure the nature of biaxial texture in the film, and the capping layer is to increase the film continuity so that any further depositions can mostly stay on the film surface. As CaF_2 is stable under air atmosphere and there is no oxidation on the surface, the substrate with this buffer layer can be stored readily for a long time. Al films were deposited subsequently in another chamber using electron beam evaporation. There was no intentional heating on the substrates during depositions.

The nature of the biaxial texture in the as-deposited Al film was verified by X-ray diffraction (XRD) and pole figure analysis. The sample deposited directly on glass without the biaxial CaF_2 buffer layer was also analyzed for comparison. The XRD 2θ plots integrated from two-dimensional (2D) XRD diffraction patterns under the same construction mechanism explained in ref 17 are shown in Figure 1a. The XRD plots can be indexed as an amorphous hump from the glass substrate, the strong diffraction peak from the {111} planes of Al for both samples, and the strong diffraction peak from {111} planes of CaF_2 for the sample with the CaF_2 buffer layer. The diffraction from other planes is weak, suggesting the strong {111} out of plane texture for both Al films. The constructed Al (111) pole figures for the films with and without the CaF_2 buffer layer are shown in Figure 1b,c, respectively. The pole intensity distribution is indicated by the color bar in Figure 1d. In Figure 1b, the pole figure of the Al film grown on the glass substrate with CaF_2 buffer layer reveals six high intensity concentration regions. Four of them coincide with the angular positions of the CaF_2 (111) poles,[17] indicating A-type epitaxial growth of Al on CaF_2. The other two are the twins of $(\bar{1}11)$ and $(11\bar{1})$ poles with (111) as the mirror plane. The twin pole of $(1\bar{1}1)$ is missing in the X-ray pole figure due to the sample shadowing on the incident or diffracted X-ray beam. Thus, the film grown with CaF_2 buffer layer is biaxially textured. In contrast, the film grown directly on glass has a fiber texture, evidenced by the (111) pole concentrated at the center and in a ring, as shown in Figure 1c. We can also see from the shape of individual pole concentration regions in Figure 1b that the out-of-plane crystallographic orientation is better confined than that of the in-plane orientations. It is estimated that the out-of-plane and in-plane orientations have angular spreads of ~5 and ~15°, respectively. The existence of twin poles is due to the possibilities of a B-type epitaxy of Al on CaF_2 (*i.e.*, a 180° rotation relationship between the two) and twinning within Al grains during growth.

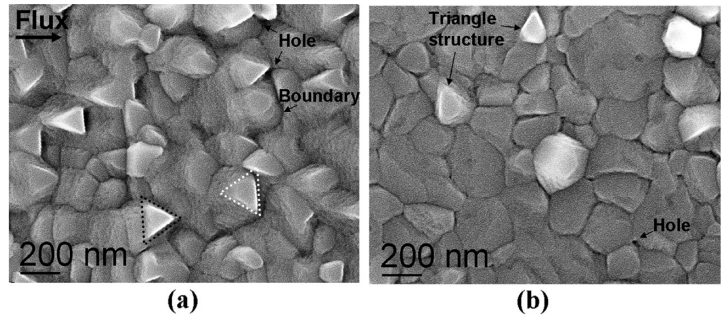

Figure 2. Top view SEM images of Al films grown on glass substrate (a) with a biaxially textured CaF_2 buffer layer and (b) without the buffer layer.

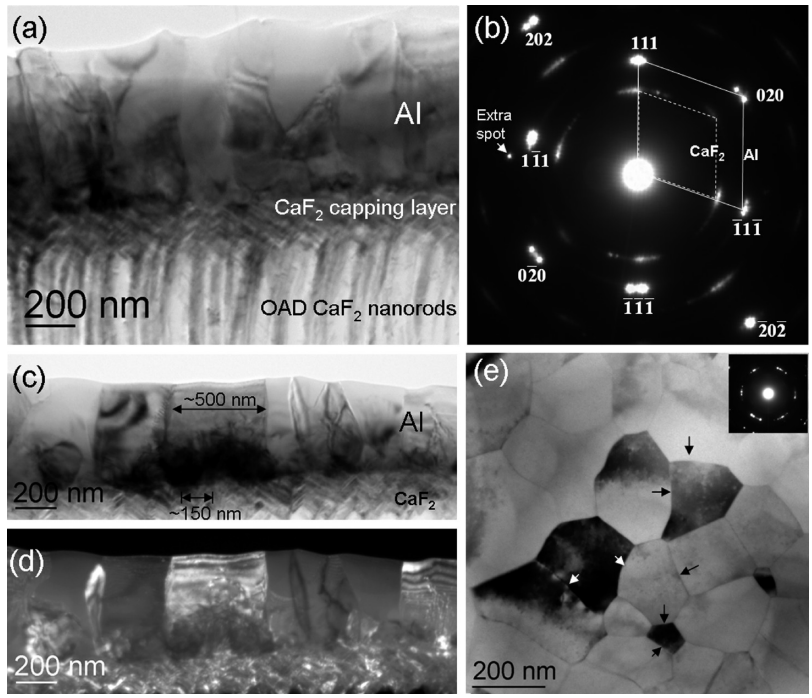

Figure 3. TEM characterization of the Al film grown on a buffer layer of biaxially textured CaF_2 nanostructures. (a) Cross section TEM image, showing the film structure. (b) Corresponding SADP of (a). (c) Bright-field and (d) dark-field TEM images, indicating the columnar grain structure in the Al film. (e) Plane view TEM image with the inset of the corresponding SADP.

Figure 2a shows the scanning electron microscopy (SEM) top view of the Al film. The projection of the OAD flux direction for the CaF_2 nanorod layer deposition is indicated by an arrow in the upper left corner of Figure 2a. We observed a number of triangle-shaped structures embedded in the film. These triangles orient either nearly along the arrow's direction (flux direction), such as the one shown by the black-dashed triangle, or in the opposite direction to the arrow, such as the one shown by the white-dashed triangle. The rest of the film is rough and contains a limited number of visible boundaries and pinholes, as indicated in the image. For comparison, the morphology of Al film grown directly on glass is shown in Figure 2b, which consists of cellular grain structure. Most boundaries between these cellular grains are wide; there are also holes in some junctions of the triboundaries. Although a few triangle-shaped structures can be observed (as indicated in the image), they have no specific orientation. As expected, Al directly grown on glass adapts a random nucleation process; therefore, the neighboring grains usually have very different crystallographic orientation and form large angle grain boundaries. The significant morphological difference between the Al film grown on the CaF_2 buffer layer and the Al film grown directly on glass is due to the crystallographic modification by the CaF_2 buffer layer. It indicates that the CaF_2 buffer layer, which possesses a crystallographic biaxial texture, can induce a preferred crystallographic orientation for the nucleation and growth of the Al film on top of it.

Transmission electron microscopy (TEM) was carried out to probe the details of Al epitaxial growth on the CaF_2 buffer layer. Figure 3a shows the cross section TEM image. From the bottom up, they are OAD CaF_2 nanorods, the CaF_2 capping layer, and the Al film. Figure 3b is the corresponding selected area diffraction pattern (SADP) from this whole region. It consists of two dot-array patterns: one is from CaF_2, in which the unit cell is connected by the dashed parallelogram, and the other from Al is connected by the solid parallelogram. The single-crystalline-like array pattern for Al confirmed the biaxial texture property of the film, consistent with the XRD pole figure analysis. The coincidence of Al crystal orientation with CaF_2 indicates the epitaxial growth of Al on CaF_2. In Figure 3b, it can also be seen that the CaF_2 diffraction spots have larger angular spread compared to those of Al, which are originated from the crystallographic randomness at the initial stages of the OAD-grown CaF_2 nanorods. The smaller angular spread in the Al diffraction spots is the result of the Al film grown on the well-established biaxial CaF_2 capping layer. Extra spots besides the dot-array pattern are sometimes observed due to the presence of small crystals grown in other crystal orientation, dislocation, and grain boundaries. The extra spots in Figure 3b, as pointed out by the arrow, may be from a small crystal in a different crystal orientation, which can be indexed as Al {200} reflection.

The nature of the Al columnar grain can be seen more clearly in Figure 3c from a thinner region of the TEM sample, and the SADP from this region is similar to Figure 3b. Figure 3d is the corresponding dark-field im-

age. From Figure 3c,d, the width of the column is estimated to be several hundred nanometers, significantly larger than the width of a single pyramidal CaF_2 cap. For example, the Al columnar grain near the center of Figure 3c,d is ~500 nm, and the CaF_2 cap under it is ~150 nm. The width of the Al columnar grain is thus almost three times that of the CaF_2 pyramidal caps. It can also be seen that there are many more boundaries in the first 200 nm thickness of Al immediately above the CaF_2 capping layer. By inheriting the crystallographic textures from the biaxial CaF_2 film, most of these boundaries of the Al film are small angle grain boundaries and many of them have disappeared as the Al film grows thicker.

Figure 3e is the plane view bright-field TEM image and the corresponding SADP. The relatively smaller Al grain size is because this region is close to the Al/CaF_2 interface, since the top part of the Al film has been milled away during the ion milling process of TEM sample preparation. We did Kikuchi diffraction analysis on a number of grains in the image. Since Kikuchi diffraction shows the three-dimensional inverse space of the crystal, it can tell the crystallographic orientation and orientation relationship among the analyzed grains. We found that the out-of-plane orientation is confined to an angle of ~5°; however, the in-plane orientation can rotate as large as ~15°. This analysis is in agreement with the estimation according to XRD pole figures as aforementioned. The in-plane rotation can also be seen from the SADP inset in Figure 3e, where the {220} diffractions appear as short arcs instead of spots. However, a number of small angle grain boundaries with less than 5° orientation difference were still identified, as pointed by the arrows in Figure 3e. The rest of the grain boundaries analyzed have an angle of ~10°.

The exposed surface plane for Al nucleation on the CaF_2 inverted pyramids can be either {111} or {110}.[17] A plane view SEM image of such CaF_2 pyramids and the corresponding schematic indicating the surface planes are shown in Figure 4a. Figure 4b is a schematic illustrating the cross section view of the structure for Al growth on CaF_2. At locations 1 and 2, the CaF_2 surface planes for Al nucleation should be close to {111} and{110}, respectively, while at location 3, where usually a CaF_2 island is located, there is no specific plane for the exposed surface. High-resolution TEM imaging was carried out to study the Al/CaF_2 interface at these different locations. As shown in Figure 4c, Al can readily have A-type epitaxial growth on CaF_2, despite their ~25% lattice mismatch and the type of exposed surface. In the image from location 1, the $\{1\bar{1}1\}$ planes of Al and CaF_2 are highlighted by parallel lines. We can see clearly the $4_{Al} \times 3_{CaF_2}$ matches in these planes. The invisible CaF_2 lattice in the high-resolution image from location 3 is due to electron irradiation during imaging, as CaF_2 is sensitive under a 200 keV electron beam.[26,27]

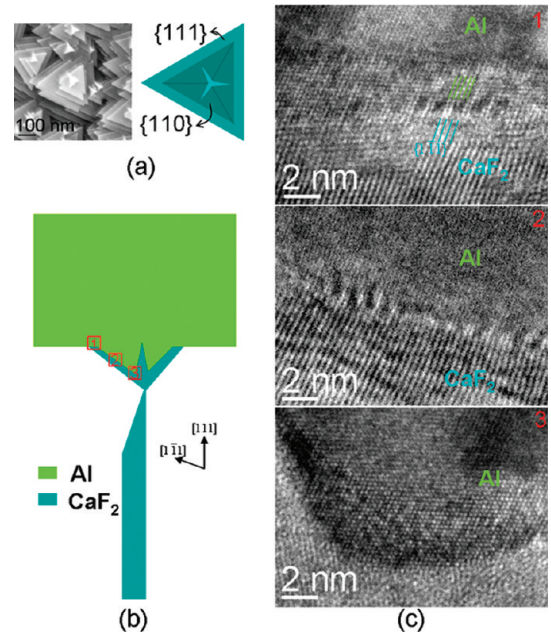

Figure 4. High-resolution TEM images of the Al/CaF_2 interface. (a) Top view SEM image of typical morphology of CaF_2 surface and the corresponding schematic illustrating the surface planes. (b) Schematic of Al on CaF_2 nanostructure illustrating the different interfacial locations for Al to nucleate. (c) High-resolution TEM images from the locations indicated in (b).

On the basis of the general epitaxial requirements, this biaxial Al film actually provides new opportunities to further prepare other biaxially textured films of materials whose lattice parameters are close to cubic Al, such as Cu, Ni, and Cr.[28−30] Furthermore, the Al film has been widely used in metal-induced crystallization of silicon and germanium for which the crystallization temperatures can be dramatically reduced. The biaxial aluminum films being used as the substrate for metal-induced crystallization can give new insights on the crystallization mechanisms and therefore pave the way for the preparation of these semiconductor films with preferred crystallographic orientations at low temperatures.

Figure 5 shows an example of Si crystallization on biaxially textured Al film. The Al layer (~100 nm) and Si layer (~400 nm) were sequentially deposited on a substrate of biaxially textured CaF_2 nanostructures. There was no intentional substrate heating during depositions; therefore, the as-deposited Al layer was biaxially textured as that in the CaF_2 film substrate, while the as-deposited Si layer was still amorphous. The sample was then annealed at 500 °C for 1 h, which resulted in the crystallization of amorphous Si. From the cross section TEM image of this annealed film and energy-dispersive X-ray (EDX) compositional analysis in Figure 5, we can see that the layers stacking from the bottom up are CaF_2 nanorods, CaF_2 capping layer, crystallized Si layer, and the layer of Al and Si mixture. The layers were confirmed through morphology, diffraction, and compositional analysis. Figure 5b,c are typical EDX spec-

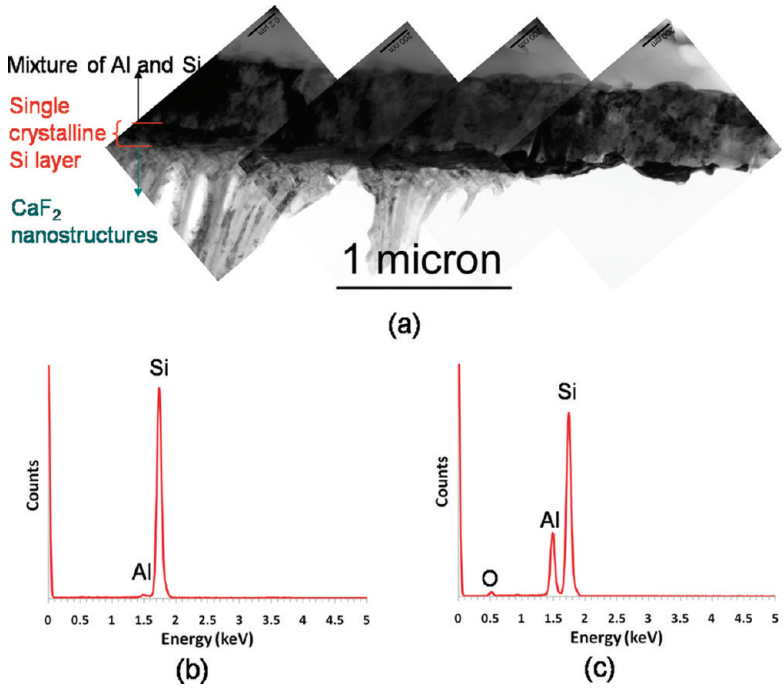

Figure 5. TEM image and compositional analysis, showing a near single-crystalline Si layer formed by crystallization of amorphous Si upon thermal annealing at 500 °C and using biaxially textured Al film as intermediate layer. (a) Cross section TEM image of the film structure after annealing. (b) EDX from the layer immediately above CaF_2 layer in (a), indicating that this layer is nearly pure Si, and therefore, the intermediate layer of Al has been replaced by Si after crystallization. (c) EDX from the topmost layer in (a), indicating the layer is a mixture of Al and Si.

tra from the crystallized Si layer and the layer of Al and Si mixture, respectively. The Al content in the crystallized Si layer is less than 1% according to this analysis. Here, it is interesting to note that the 100 nm Al biaxial layer has been replaced by the crystalline Si layer upon thermal annealing. Most importantly, this Si layer is nearly single crystalline across the 4 μm analysis region. The formation of the near single-crystalline Si layer after crystallization suggests that there is a specific crystallographic orientation relationship between Al and Si during their layer exchange and the crystallization process of amorphous Si. While more research is needed to understand this exceptional crystallization mechanism, this current work has already exhibited a potential for the fabrication of Si thin film devices on glass. What's more, the understanding of the mechanism may provide insight to further reduce the crystallization temperature, making it possible to fabricate crystalline Si film on flexible substrates, like polymers, with stability temperature lower than 350 °C.

CONCLUSIONS

A biaxially textured Al film has been obtained on glass substrate with biaxially textured CaF_2 nanostructures as the buffer layer. The formation of biaxial texture in the Al film was through direct epitaxy on the facets of CaF_2 nanocrystals. The room temperature heteroepitaxy of Al film on biaxially textured CaF_2 nanostructures has been characterized using high-resolution TEM, XRD, and SEM techniques. The grain size of Al increases with the film thickness, which was observed to be several hundred nanometers in an 800 nm thick film. We suggest that this strategy can be possibly adopted to grow other types of biaxial metal films for applications that require fine quality crystalline metals to achieve desirable properties. Furthermore, the biaxial Al film itself can be utilized as a substrate to further grow biaxial materials, particularly the biaxial semiconductors. An example of such application on the preparation of a single-crystalline Si layer is demonstrated.

EXPERIMENTAL SECTION

CaF_2 layers were thermally evaporated onto glass substrates in a chamber with vacuum level in 10^{-7} Torr. Al and Si layers were ebeam evaporated in a chamber with vacuum level in 10^{-7} Torr. XRD and pole figure analysis was carried out in a Bruker D8 Discover diffractometer (Cu target, wavelength = 0.15405 nm) using an area detector. Field emission scanning electron microscopy (Carl Zeiss Supra SEM 1550) was used for morphological observations. TEM was carried out in JEOL 2010 200 kV TEM. The TEM samples were prepared through conventional methods. For cross section samples, the steps included the following: (a) cut the sample into ~2 mm × 3 mm slots; (b) then glue two sample slots together with film sides face to face using epoxy; (c) mechanically grind the bulk across the interface until ~10 μm thick material is left, and use a Cu aperture grid to reinforce this foil for easy handling; (d) ion mill until electron transparency. For plane view TEM samples, the steps were to (a) cut the sample into ~3 mm × 3 mm slots; (b) mechanically grind the sample from substrate side until ~10 μm, use a Cu aperture grid to reinforce the foil; (c) ion mill from the substrate side,

maintaining a weak ion beam to mill the film side in order to remove the material redeposited, until electron transparency. EDX compositional analysis was processed in an Oxford instrument that attached to the TEM column.

Acknowledgment. We would like to thank NSF-NIRT Award 0506738 for support.

REFERENCES AND NOTES

1. Wang, C. P.; Do, K. B.; Beasley, M. R.; Geballe, T. H.; Hammond, R. H. Deposition of In-Plane Textured MgO on Amorphous Si_3N_4 Substrates by Ion-Beam-Assisted Deposition and Comparisons with Ion-Beam-Assisted Deposited Yttria-Stabilized-Zirconia. *Appl. Phys. Lett.* **1997**, *71*, 2955–2957.
2. Bauer, M.; Semerad, R.; Kinder, H. YBCO Films on Metal Substrates with Biaxially Aligned MgO Buffer Layers. *IEEE Trans. Appl. Supercond.* **1999**, *9*, 1502–1505.
3. Groves, J. R.; Arendt, P. N.; Foltyn, S. R.; De Paula, R. F.; Peterson, E. J.; Holesinger, T. G.; Coulter, J. Y.; Springer, R. W.; Wang, C. P.; Hammond, R. H. Ion-Beam Assisted Deposition of Bi-axially Aligned MgO Template Films for YBCO Coated Conductors. *IEEE Trans. Appl. Supercond.* **1999**, *9*, 1964–1966.
4. Chudzik, M. P.; Koritala, R. E.; Luo, L. P.; Miller, D. J.; Balachandran, U.; Kannewurf, C. R. Mechanism and Processing Dependence of Biaxial Texture Development in Magnesium Oxide Thin Films Grown by Inclined-Substrate Deposition. *IEEE Trans. Appl. Supercond.* **2001**, *11*, 3469–3472.
5. Ma, B.; Li, M.; Koritala, R. E.; Fisher, B. L.; Markowitz, A. R.; Erck, R. A.; Dorris, S. E.; Miller, D. J.; Balachandran, U. Biaxially Aligned Template Films Fabricated by Inclined-Substrate Deposition for YBCO-Coated Conductor Applications. *IEEE Trans. Appl. Supercond.* **2003**, *13*, 2695–2698.
6. Foltyn, S. R.; Arendt, P. N.; Jia, Q. X.; Wang, H.; MacManus-Driscoll, J. L.; Kreiskott, S.; DePaula, R. F.; Stan, L.; Groves, J. R.; Dowden, P. C. Strongly Coupled Critical Current Density Values Achieved in $Y1Ba^2Cu^3O^{7-\delta}$ Coated Conductors with Near-Single-Crystal Texture. *Appl. Phys. Lett.* **2003**, *82*, 4519–4521.
7. Goyal, A.; Paranthaman, M. P.; Schoop, U. The RABiTS Approach: Using Rolling-Assisted Biaxially Textured Substrates for High-Performance YBCO Superconductors. *MRS Bull.* **2004**, *8*, 552–561.
8. Xu, Y.; Lei, C. H.; Ma, B.; Evans, H.; Efstathiadis, H.; Rane, M.; Massey, M.; Balachandran, U.; Bhattacharya, R. Growth of Textured MgO through E-Beam Evaporation and Inclined Substrate Deposition. *Supercond. Sci. Technol.* **2006**, *19*, 835–843.
9. Xiong, J.; Chen, Y.; Qiu, Y.; Tao, B.; Qin, W.; Cui, X.; Tang, J.; Li, Y. Deposition of High-Textured Buffer Layers for YBCO Coated Conductors by All-IPAT-Process. *Physica C* **2007**, *454*, 56–60.
10. Findikoglu, A. T.; Choi, W.; Matias, V.; Holesinger, T. G.; Jia, Q. X.; Peterson, D. E. Well-Oriented, High-Carrier-Mobility Silicon Thin Films on Non-Single-Crystalline Substrates. *Adv. Mater.* **2005**, *17*, 1527–1531.
11. Yuan, W.; Tang, F.; Li, H. F.; Parker, T.; Licausi, N.; Lu, T.-M.; Bhat, I.; Wang, G.-C.; Lee, S. Biaxial CdTe/CaF_2 Films Growth on Amorphous Surface. *Thin Solid Films* **2009**, *517*, 6623–6628.
12. Licausi, N.; Yuan, W.; Tang, F.; Parker, T.; Li, H. F.; Wang, G.-C.; Lu, T.-M; Bhat, I. Growth of CdTe Films on Amorphous Substrates Using CaF_2 Nanorods as a Buffer Layer. *J. Electron. Mater.* **2009**, *38*, 1600–1604.
13. Gaire, C.; Clemmer, P. C.; Li, H. F.; Parker, T. C.; Snow, P.; Bhat, I.; Lee, S.; Wang, G.-C.; Lu, T.-M. Small Angle Grain Boundary Ge Films on Biaxial CaF_2/Glass Substrate. *J. Cryst. Growth* **2010**, *312*, 607–610.
14. Aboelfotoh, M. A. Crystal Structure of Evaporated MgO Films on Amorphous and Polycrystalline Substrates. *J. Vac. Sci. Technol.* **1973**, *10*, 621–628.
15. Mahieu, S.; Ghekiere, P.; Depla, D.; Gryse, R. D. Biaxial Alignment in Sputter Deposited Thin Films. *Thin Solid Films* **2006**, *515*, 1229–1249.
16. Brewer, R. T.; Atwater, H. A. Rapid Biaxial Texture Development During Nucleation of MgO Thin Films During Ion-Beam-Assisted Deposition. *Appl. Phys. Lett.* **2002**, *80*, 3388–3390.
17. Li, H. F.; Parker, T.; Tang, F.; Wang, G.-C.; Lu, T.-M.; Lee, S. Biaxially Oriented CaF_2 Films on Amorphous Substrates. *J. Cryst. Growth* **2008**, *310*, 3610–3614.
18. Krishnan, R.; Parker, T.; Lee, S.; Lu, T.-M. The Formation of Vertically Aligned Biaxial Tungsten Nanorods Using a Novel Shadowing Growth Technique. *Nanotechnology* **2009**, *20*, 465609.
19. Nast, O.; Puzzer, T.; Koschier, L. M.; Sproul, A. B.; Wenham, S. R. Aluminum-Induced Crystallization of Amorphous Silicon on Glass Substrates above and below the Eutectic Temperature. *Appl. Phys. Lett.* **1998**, *73*, 3214–3216.
20. Ishikawa, Y.; Nakamura, A.; Uraoka, Y.; Fuyuki, T. Polycrystalline Silicon Thin Film for Solar Cells Utilizing Aluminum Induced Crystallization Method. *Jpn. J. Appl. Phys.* **2004**, *43*, 877–881.
21. Ornaghi, C.; Beaucarne, G.; Poortmans, J.; Nijs, J.; Mertens, R. Aluminum-Induced Crystallization of Amorphous Silicon: Influence of Materials Characterization on The Reaction. *Thin Solid Films* **2004**, *451−452*, 476–480.
22. Wang, Z.; Jeurgens, L. P. H.; Wang, J. Y.; Mittemeijer, E. J. High-Resolution Transmission-Electron-Microscopy Study of Ultrathin Al-Induced Crystallization of Amorphous Si. *J. Mater. Res.* **2009**, *24*, 3294–3299.
23. Cho, C.-C.; Liu, H.-Y.; Tsai, H.-L. Epitaxial Growth of An Al/CaF2/Al/Si(111) Structure. *Appl. Phys. Lett.* **1992**, *61*, 270–272.
24. Lu, T.-M.; Bai, P.; Yapsir, A.-S.; Chang, P.-H.; Shaffner, T. J. Direct Observation of An Incommensurate Solid−Solid Interface. *Phys. Rev. B* **1989**, *39*, 9584–9586.
25. Shusterman, Y. V.; Yakovlev, N. L.; Dovidenko, K.; Schowalter, L. J. Growth and Structure of Epitaxial Al and Cu Films on CaF_2. *Thin Solid Films* **2003**, *443*, 23–27.
26. Kogure, T.; Saiki, K.; Konno, M.; Kamino, T. HRTEM and EELS Studies of Reacted Materials from CaF_2 by Electron Beam Irradiation. *Mater. Res. Soc. Symp. Proc.* **1997**, *504*, 183–188.
27. Ding, T. H.; Zhu, S.; Wang, L. M. *In Situ* TEM Study of Electron Beam Stimulated Organization of Three-Dimensional Void Superlattice in CaF_2. *Mater. Res. Soc. Symp. Proc.* **2005**, *849*, K8.9.1.
28. Shusterman, Y. V.; Yakovlev, N. L.; Schowalter, L. J. Ultra-Thin Epitaxial Al and Cu Films on CaF_2/Si(111). *Appl. Surf. Sci.* **2001**, *175−176*, 27–32.
29. Yandouzi, M.; Toth, L.; Vasudevan, V.; Cannaerts, M.; Haesendonck, C. V.; Schryvers, D. Epitaxial Ni−Al Thin Films on NaCl Using a Ag Buffer Layer. *Philos. Mag. Lett.* **2000**, *80*, 719–724.
30. Kingetsu, T.; Kamada, Y.; Yamamoto, M. Molecular-Beam Epitaxial Growth of (001) Cr/Al/Cr/Al Quadrilayer Superlattice Containing One-Monolayer-Thick Cr Layers. *Jpn. J. Appl. Phys.* **2000**, *39*, 4174–4175.